Title: Long-Term Risk and Prediction of Progression in Primary Angle Closure Suspect

Running title: Long-Term Risk and Prediction of PACS Progression

Authors: Yixiong Yuan, MD [1,2,3,*], Ruilin Xiong, MD, PhD [1,2,3,*], Wei Wang, MD, PhD [1,2,3,4,†], Benjamin Y. Xu, MD, PhD [5], Chimei Liao, MD, PhD [1,2,3], Shaopeng Yang, MD [1,2,3], Cong Li, MD [1,2,3], Jian Zhang, MPH [1,2,3], Qiuxia Yin, MPH [1,2,3], Yingfeng Zheng, MD, PhD [1,2,3], David S. Friedman, MD, PhD [6], Paul J. Foster, PhD [7], Mingguang He, MD, PhD [1,8]

Affiliations:
1. State Key Laboratory of Ophthalmology, Zhongshan Ophthalmic Center, Sun Yat-sen University, Guangzhou, China
2. Guangdong Provincial Key Laboratory of Ophthalmology and Visual Science, Guangzhou, China
3. Guangdong Provincial Clinical Research Center for Ocular Diseases, Guangzhou, China
4. Hainan Eye Hospital and Key Laboratory of Ophthalmology, Zhongshan Ophthalmic Center, Sun Yat-sen University, Haikou, China
5. Roski Eye Institute, Keck School of Medicine, University of Southern California, Los Angeles, California
6. Department of Ophthalmology, Massachusetts Eye and Ear, Harvard Medical School, Boston
7. NIHR Biomedical Research Centre at Moorfields Eye Hospital and UCL Institute of Ophthalmology, London, United Kingdom
8. Experimental Ophthalmology, The Hong Kong Polytechnic University, Hong Kong, China
* Y. Y. and R. X. contributed equally to this work.
† Corresponding author: Wei Wang, MD, PhD, State Key Laboratory of Ophthalmology, Zhongshan Ophthalmic Center, Sun Yat-sen University, Guangzhou 510060, China (wangwei@gzzoc.com).

Key Words:
primary angle closure suspect, primary angle closure, risk factor, prediction model, anterior segment optical coherence tomography

Word count: Abstract 411; **Text** 3253

Tables: 4;

Key Points

Question: Can ophthalmic examinations at baseline be used to predict the 14-year risk of progression to primary angle closure (PAC) in primary angle closure suspect (PACS) eyes?

Findings: In this cohort study of data from 377 PACS eyes of 377 participants from the Zhongshan Angle Closure Prevention trial, logistic regression models that included baseline intraocular pressure and central and limbal anterior chamber depths had moderate performance in predicting 14-year risk of progression from PACS to PAC.

Meaning: Findings of this study suggest that factors at baseline may be used for primary risk stratification of eyes at high risk of PAC within 14 years, which can aid in customizing PACS management.

Abstract

Importance: Identifying primary angle closure suspect (PACS) eyes at risk of angle closure is crucial for its management. However, the risk of progression and its prediction are still understudied in long-term longitudinal studies about PACS. Objective: To explore baseline predictors and develop prediction models for the 14-year risk of progression from PACS to primary angle closure (PAC).

Design, Setting, and Participants: This cohort study involved participants from the Zhongshan Angle Closure Prevention trial who had untreated eyes with PACS. Baseline examinations included tonometry, ultrasound A-scan biometry, and anterior segment optical coherence tomography (AS-OCT) under both light and dark conditions. Primary angle closure was defined as peripheral anterior synechiae in 1 or more clock hours, intraocular pressure (IOP) greater than 24 mm Hg, or acute angle closure. Based on baseline covariates, logistic regression models were built to predict the risk of progression from PACS to PAC during 14 years of follow-up.

Results: The analysis included 377 eyes from 377 patients (mean [SD] patient age at baseline, 58.28 [4.71] years; 317 females [84%]). By the 14-year follow-up visit, 93 eyes (25%) had progressed from PACS to PAC. In multivariable models, higher IOP (odds ratio [OR], 1.14 [95% CI, 1.04-1.25] per 1-mm Hg increase), shallower central anterior chamber depth (ACD; OR, 0.81 [95% CI, 0.67-0.97] per 0.1-mm increase), and shallower limbal ACD (OR, 0.96 [95% CI, 0.93-0.99] per 0.01 increase in peripheral corneal thickness) at baseline were associated with an increased 14-year risk of progression from PACS to PAC. As for AS-OCT measurements, smaller light-room trabecular-iris space area (TISA) at 500 μm from the scleral spur (OR, 0.86 [95% CI, 0.77-0.96] per 0.01-mm^2 increase), smaller light-room angle recess area (ARA) at 750 μm from the scleral spur (OR, 0.93 [95% CI, 0.88-0.98] per 0.01-mm^2 increase), and smaller dark-room TISA at 500 μm (OR, 0.89 [95% CI, 0.80-0.98] per 0.01-mm^2 increase) at baseline were identified as predictors for the 14-year risk of progression. The prediction models based on IOP and central and limbal ACDs

showed moderate performance (area under the receiver operating characteristic curve, 0.69; 95% CI, 0.63-0.75) in predicting progression from PACS to PAC, and inclusion of AS-OCT metrics did not improve the model's performance.

Conclusions and Relevance: This cohort study suggests that higher IOP, shallower central and limbal ACDs, and smaller TISA at 500 μm and light-room ARA at 750 μm may serve as baseline predictors for progression to PAC in PACS eyes. Evaluating these factors can aid in customizing PACS management.

Introduction

Primary angle-closure glaucoma (PACG) is one of the major causes of blindness, affecting more than 20 million patients worldwide.[1] In China, PACG accounts for about half of the population with glaucoma and the majority of bilateral glaucoma-relevant blindness.[2] Characterized by appositional angle closure, primary angle closure suspect (PACS) is the earliest stage of primary angle closure diseases, which can finally progress to primary angle closure (PAC) and PACG.[3,4] Early laser peripheral iridotomy (LPI) has been associated with improvement in the clinical course of angle closure. However, due to the low rate of progression of PACS, findings from the Zhongshan Angle Closure Prevention (ZAP) trial and Singapore Asymptomatic Narrow Angles Laser Iridotomy Study do not support the widespread practice of LPI based on the current definition of PACS.[5,6] To improve cost-effectiveness and avoid unnecessary treatment, stratifying patients with PACS eyes at higher risk of progression is expected to guide prophylactic intervention in the early stage.

Anterior segment optical coherence tomography (AS-OCT) is a quantitative, non-contact tool for in vivo assessment of the anterior chamber angle (ACA). Based on AS-OCT results, previous reports on the ZAP trial suggested that smaller angle width, iris curvature, and light-to-dark changes of the iris were associated with an increased 6-year risk of progression from PACS to PAC.[7,8] However, angle closure diseases are more prevalent in the elderly,[9,10] and those reports[7,8] also found that aging was a risk factor for progression in PACS eyes. Recent results from the extended follow-up of ZAP trial participants indicated that in untreated PACS eyes, the number of those with progression 7 to 14 years after baseline was double that after the first 6 years.[11] The greater rate of progression of PACS eyes observed in the extended follow-up suggests that identifying eyes at risk of progression to PAC or PACG over a longer time frame is warranted.

This study aimed to evaluate baseline risk factors associated with the 14-year risk of progression from PACS to PAC in untreated PACS eyes. To provide practical tools for decision-making at initial diagnosis, prediction models were developed to help identify PACS eyes at higher risk of progression during the long term.

Methods

The ZAP trial was a single-center randomized clinical trial carried out at Zhongshan Ophthalmic Center. Details of the study design were approved by the Center's Ethical Committee and registered previously (ISRCTN45213099).[12] This study adhered to tenets of the Declaration of Helsinki[13] and written informed consent was obtained from participants before each visit. This study was reported according to the Strengthening the Reporting of Observational Studies in Epidemiology (STROBE) reporting guideline.[14]

Study Participants: Since 2008, 11 991 urban residents aged 50 to 70 years were screened for bilateral PACS, which is defined as a nonvisible pigmented trabecular meshwork spanning 6 or more clock hours under static gonioscopic examination without peripheral anterior synechiae (PAS), history of acute angle closure (AAC), intraocular pressure (IOP) greater than 21 mm Hg, or glaucomatous neuropathy. Participants with IOP elevation greater than 15 mm Hg after 15-minute dark room prone provocative testing (DRPPT) were considered as being at risk for AAC and excluded. Participants with a history of intraocular trauma or surgery were also excluded. At baseline, 889 eligible participants were enrolled and received LPI in 1 randomly selected eye. Follow-up visits were scheduled at 2 weeks and 0.5, 1.5, 3, 4.5, 6, and 14 years after baseline. Primary angle closure, a combined end point consisting of PAS no less than 1 clock hour in any quadrant, IOP greater than 24 mm Hg at 2 separate visits, and AAC, was the primary outcome. Only untreated PACS eyes that progressed to PAC and that were evaluated at the 14-year visit were included in current analyses. Transportation subsidies were provided for participants to improve compliance with follow-up.

Examinations at Baseline: Limbal anterior chamber depth (ACD) was measured by the brightest and narrowest slit light beam perpendicular to the temporal limbus and viewed from the nasal side as corresponding percentages of the peripheral corneal thickness (PCT).[15] Static gonioscopy was performed using a Goldmann-type single-mirror goniolens under low ambient luminance (<1 lux). Based on the 5-level Shaffer grading system, angle width was assessed in each quadrant with a 1-mm– wide slit light beam. In the case of an excessively bowed iris, minimal tilting (≤10°) of the gonioprism was allowed to visualize the ACA. The total angle width score was calculated by summing the Shaffer grading from all 4 quadrants (0-16, with higher points representing larger angle width). If the trabecular meshwork was still not visible under static examination, dynamic indentation gonioscopy using a Sussman type 4-mirror goniolens was performed to determine PAS, defined as persistent adhesion between the iris and corneal-scleral wall anterior to the scleral spur despite indentation. Gonioscopy was performed by an experienced glaucoma specialist (W.W.) with good interindividual agreement with previous examiners (weighted κ > 0.80). At each visit, 3 IOP measurements were obtained by Goldmann applanation tonometry and averaged. In DRPPT, an applanation tonometer (Tono-Pen XL; Medtronic) was used to measure IOP before and after the patient lay face down for 15 minutes in a dark room. Axial length, central ACD, and lens thickness were measured by ultrasound A-scan biometry (CineScan A/B scan; Quantel Medical).

Anterior Segment Optical Coherence Tomography at Baseline: Anterior segment optical coherence tomography (Visante; Carl Zeiss Meditec, Inc) was performed at baseline to quantify the ACA and other anterior segment structures. The procedure was first performed in the dark condition (<1 lux; hereafter, dark-room AS-OCT) and then in the light condition (350-400 lux; hereafter, light-room AS-OCT). Only horizontal scans were analyzed to avoid obstruction of the ACA by eyelids. Quantitative analysis of AS-OCT images was performed by an experienced grader (C.L.) using the custom software, Zhongshan Angle Assessment Program.[16]

Briefly, the program automatically segmented the anterior chamber structures and exported measurement results after scleral spurs were manually marked by human graders. This study included the following parameters (eFigure 1 in Supplement 1): anterior chamber area, anterior chamber width, lens vault, pupil diameter, angle opening distance (AOD) at 500 μm from the scleral spur, trabecular-iris space area (TISA) at 500 μm from the scleral spur, angle recess area (ARA) at 750 μm from the scleral spur, iris thickness at 750 μm from the scleral spur, iris area, and iris curvature. Light-to-dark changes in AS-OCT metrics were calculated by subtracting dark-room values from corresponding light-room values.

Statistical Analysis: Demographic and clinical characteristics at baseline were compared between PACS eyes with and without PAC progression. Univariable logistic regression models were built to assess associations between baseline covariates and the 14-year risk of progression from PACS to PAC, with results reported as odds ratios (ORs) and 95% CIs. Covariates with P < .10 were included in multivariable logistic regression models. Due to collinearity, light-room AOD at 500 μm, TISA at 500 μm, and ARA at 750 μm were analyzed separately in multivariable models A, B, and C. In sensitivity analyses, light-room AS-OCT metrics were replaced by dark-room metrics, which formed multivariable models D, E, and F. Risk factors with P < .05 in multivariable models were further analyzed to develop prediction models for progression in PACS eyes within 14 years of follow-up. Based on the cumulative 14-year incidence rate of PAC in untreated PACS reported previously (105 of 427 eyes [25%]),[11] estimated risks of progression were arbitrarily stratified into 3 levels (<20%, 20%-30%, and >30%). For predictors and prediction models, the observed incidence rates of progression and corresponding cutoff values were reported by risk levels. To evaluate discrimination abilities between prediction models, areas under the receiver operating characteristics curve (AUROC) were compared using Delong tests. To reflect model calibration, estimated probabilities and observed proportions of progression were compared using Hosmer-Lemeshow tests. Moreover, net reclassification improvement and integrated discrimination improvement were calculated to evaluate reclassification values. Statistical analyses

were performed by Stata, version 15.1 (StataCorp LLC) and R, version 4.1.2 (R Project for Statistical Computing). All P values were 2-sided but were not adjusted for multiple analyses.

Results

Among 889 untreated PACS eyes, 388 eyes were lost to follow-up and 20 eyes were censored before the 14-year visit due to death. In addition, 54 and 12 eyes were excluded because of cataract surgery or LPI before the primary outcome, respectively. With 38 eyes further excluded due to unavailable ultrasound A-scan or AS-OCT results, 377 eligible untreated PACS eyes of 377 patients (mean [SD] age at baseline, 58.28 (4.71) years; 317 females [84%] and 60 males [16%]) were included in the analysis. Differences in age, central ACD, lens thickness, and DRPPT were found between eligible eyes and excluded eyes at baseline (eTable 1 in Supplement 1). During 14 years of follow-up, 93 of 377 untreated PACS eyes (25%) progressed to PAC (Table 1), with 64 (69%) diagnosed at the 14-year visit and a higher rate of identification during the extended follow-up (1-6 years: 4.83 cases/y; 7-14 years: 8.00 cases/y) (eTable 2 in Supplement 1). An IOP greater than 24 mm Hg and AAC were observed in 6 and 3 eyes, respectively. After the 6-year visit, only 1 case of IOP elevation was found, and no cases of AAC were found. Through the 14 years, 4 eyes were diagnosed with PACG and referred for further treatment.

Table 1 shows that eyes with progression to PAC had higher IOP, narrower total angle width, thicker lens, and shallower central and limbal ACDs at baseline. Moreover, baseline anterior chamber area, AOD at 500 μm, TISA at 500 μm, and ARA at 750 μm were smaller in eyes with progression to PAC under both light and dark conditions. In multivariable model A (adjusted for baseline covariates with a P < .10 in univariable models and including AOD at 500 μm) (Table 2), higher IOP (OR, 1.14 [95% CI, 1.04-1.25] per 1-mm Hg increase), shallower central ACD (OR, 0.81 [95% CI, 0.67-0.97] per 0.1-mm increase), and shallower limbal ACD (OR, 0.96 [95% CI, 0.93-0.99] per 0.01-PCT increase) at baseline were associated with an increased 14-

year risk of progression to PAC. With light-room AOD at 500 μm replaced by light-room TISA at 500 μm (multivariable model B) (OR, 0.86 [95% CI, 0.77-0.96] per 0.01-mm^2 increase) and light-room ARA at 750 μm (multivariable model C) (OR, 0.93 [95% CI, 0.88-0.98] per 0.01-mm^2 increase), IOP and central ACD remained associated with the 14-year risk of progression in PACS eyes (Table 3). In multivariable models D, E, and F (replacing light-room AS-OCT metrics by dark-room metrics), baseline dark-room TISA at 500 μm (OR, 0.89 [95% CI, 0.80-0.98] per 0.01-mm^2 increase) was the only dark-room AS-OCT metric associated with the 14-year risk of progression in PACS eyes. Light-to-dark changes of AS-OCT were not associated with the 14-year risk of progression in either univariable or multivariable models (eTables 3-5 in Supplement 1).

Based on multivariable analyses, risk factors with P < .05 were included in prediction models (Table 4). Prediction model A included IOP and central and limbal ACDs. Prediction model B included IOP, central ACD, and light-room TISA at 500 μm. Prediction model C included IOP, central ACD, and light-room ARA at 750 μm. Prediction model D included IOP, central ACD, and dark-room TISA at 500 μm. Prediction models E and F were omitted because their components were consistent with those of prediction model A. With estimated risks arbitrarily categorized into 3 strata (<20%, 20%-30%, and >30%), the 14-year incidence rate of progression from PACS to PAC increased with risk levels predicted by IOP (<13, 13-17, and >17 mm Hg), central ACD (>2.66, 2.43-2.66, and <2.43 mm), light-room TISA at 500 μm (>0.08, 0.06-0.08, and <0.06 mm^2), light-room ARA at 750 μm (>0.18, 0.12-0.18, and <0.12 mm^2), and dark-room TISA at 500 μm (>0.06, 0.03-0.06, and <0.03 mm^2), but not limbal ACD (eTables 6-9 in Supplement 1). Compared with IOP and central and limbal ACDs, prediction model A provided better discrimination in predicting progression from PACS to PAC (AUROC, 0.69 [95% CI, 0.63-0.75]), and no difference was found in accuracy among prediction models A, B, C, and D (eFigure 2 and eTable 10 in Supplement 1). Model calibration was adequate in this study, with χ2 < 20 found in all 4 models (eFigure 3 in Supplement 1). Reclassification analyses

suggested that the accuracy of risk prediction was comparable in the 4 prediction models (eTable 11 in Supplement 1).

Discussion

In untreated PACS eyes, higher IOP and shallower central and limbal ACDs at baseline were associated with an increased 14-year risk of progression from PACS to PAC. Among AS-OCT metrics at baseline, smaller light-room TISA at 500 μm, light-room ARA at 750 μm, and dark-room TISA at 500 μm were identified as key predictors for progression. Based on IOP and central and limbal ACDs, logistic regression models showed moderate performance in predicting the long-term risk of progression in untreated PACS eyes. With limbal ACD replaced by AS-OCT parameters, alternative models had comparable performance in predicting progression from PACS to PAC within 14 years.

In the present study, we found that baseline IOP was higher in PACS eyes that progressed to PAC, consistent with the findings of the Singapore Epidemiology of Eye Diseases Study.[17] Given that angle closure can impede aqueous outflow and elevate IOP, it is intuitive that the risk of progression from PACS to PAC increases with higher baseline IOP. Central ACD is another established risk factor in the development of angle closure disease. As a key factor of the anterior chamber, central ACD reflects the contribution of lens position to angle crowding.[18] In accordance with this finding, previous studies reported that central ACD was negatively associated with the increased incidence of PACS and PAC over 5 to 10 years in the Chinese PACS population.[19,20] Additionally, the present study found that limbal ACD was also a predictor for the progression from PACS to PAC during the long term. A meta-analysis suggested that limbal ACD performed as well as sophisticated anterior segment imaging in diagnosing occludable angles.[21] Although its performance is relatively low in community-based screening,[22] limbal ACD may be considered as an alternative barometer for the prognosis of PACS, especially in the absence of imaging results.

Extensive studies have found that AS-OCT examination was particularly useful for diagnosing and monitoring angle closure diseases. Su et al[23] suggested that AOD, TISA, and ARA were smaller in PAS eyes and weakly associated with PAS extent. Xu et al[24] found that TISA and ARA were smaller in PAC and PACG eyes compared with PACS eyes. Longitudinal studies reported that smaller AOD and TISA at baseline were risk factors in PACS incidence over 4 to 5 years of follow-up.[25,26] Previous results from the ZAP trial suggested that PACS eyes with smaller AOD and TISA at baseline had a higher risk of progression over 6 years.[7,8] The current study supports the previous findings and confirms the importance of AS-OCT over a longer time frame. After adjustments for IOP and central and limbal ACDs, the area of ACA measured by AS-OCT provides additional information about the progression from PACS to PAC. Different from linear measurements, area parameters consider the irregular shape of the iris' anterior surface and reflect the width of ACA from a 2-dimensional perspective, which may explain why TISA at 500 μm and ARA at 750 μm, rather than AOD at 500 μm, remained associated with progression after data adjustments.

To date, dark-room AS-OCT has been more commonly performed in previous studies. However, recent studies have challenged this practice by reporting that AOD and TISA measured in light but not in dark conditions were smaller in eyes with PAS.[27,28] In this study, we found that both dark-room and light-room TISA at 500 μm were associated with progression from PACS to PAC during the long term. Given that anterior chamber structures change with luminance, performing light-room AS-OCT is more complicated than dark-room ones. As a supplement, light-room AS-OCT should not be neglected because it provides information about wider ACAs at physiological states.[29,30] More efforts are needed to standardize the measurement condition and determine its clinical values. A previous study found that eyes with occludable angles had a slower speed of pupillary constriction,[31] indicating that dynamic changes of iris volume from light to dark may be compromised and contribute to angle closure.[32] Another study[7] found that eyes with

decreased light-to-dark changes of the iris were more likely to develop angle closure within 5 to 6 years. However, associations between iris-related parameters and progression from PACS to PAC within 14 years were not found in this study, which may be attributed to the low risk of progression and a high rate of loss to follow-up.

Despite prophylactic use of LPI for angle closure, its widespread use has not been recommended, as 6-year ZAP trial reports[6] found a low rate of progression from PACS to PAC. To identify high-risk PACS eyes requiring intervention, several prediction models based on AS-OCT have been developed, which had a moderate performance over 5 to 6 years (AUROC 0.70-0.83).[7,8,26] With the follow-up period extended to 14 years in the present study, 64 extra eyes with progression were observed in total. Considering that the long-term risk of progression is relatively low and most cases with progression start as PAS, this study supports previous conclusions that widespread intervention is not recommended in community-based PACS populations at low risk of angle closure, especially for those with younger age and wider angles. Nonetheless, more eyes with progression observed within our extended follow-up still warrant monitoring and prophylaxis for the long-term risk of progression in PACS. Contrary to expectation, this study finds that sophisticated AS-OCT does not perform better than basic ophthalmic examinations, such as measuring IOP and central and limbal ACDs, from a long-term perspective. Given that AS-OCT is sometimes not readily available in clinical practice, our findings suggest that AS-OCT is not necessary for the evaluation of PACS eyes, and examinations without optical coherence tomography are sufficient in the primary assessment for risk of progression during the long term.

Limitations: There are several limitations to this study. First, 512 of 889 untreated control eyes were excluded during 14 years of follow-up. Compared with eyes eligible for analysis, excluded eyes had shallower central ACD and thicker lenses, which inevitably introduced selection bias in this study. Second, younger age and wider angles in ZAP trial participants recruited from large-scale screening led to a lower rate of PAC progression compared with that in hospital-based studies.[5]

Interpretation of findings from the present study should be cautious and restricted to community-based population at relatively low risk of progression. Third, all ZAP trial participants were urban residents in South China, which further limits generalizability of these results. More cohorts are needed to validate our findings in populations with different ethnic backgrounds and those living in areas with insufficient access to medical services. Finally, the Visante AS-OCT has become outdated and been replaced by swept source AS-OCT.[33] Three-dimensional and high-resolution measurement of the anterior chamber is expected to improve our models' predictive performance.

Conclusions

In this cohort study, several factors including higher IOP, shallower central and limbal ACDs, smaller TISA at 500 μm, and smaller light-room ARA at 750 μm at baseline were associated with an increased risk of progression from PACS to PAC over 14 years. Both AS-OCT measurements and ophthalmic examinations not using this technique allowed for the primary identification of PACS eyes at higher risk of PAC progression. Routine follow-up should be scheduled and early intervention with LPI or cataract surgery could be considered for management of high-risk PACS eyes. Further efforts are needed to validate these findings and improve the predictive performance of our models.

References

1. Tham YC, Li X, Wong TY, Quigley HA, Aung T, Cheng CY. Global prevalence of glaucoma and projections of glaucoma burden through 2040: a systematic review and meta-analysis. *Ophthalmology*. 2014;121(11):2081-2090. Medline:24974815 doi:10.1016/j.ophtha.2014.05.013

2. Foster PJ, Johnson GJ. Glaucoma in China: how big is the problem? *Br J Ophthalmol*. 2001;85(11):1277-1282. Medline:11673287 doi:10.1136/bjo.85.11.1277

3. Foster PJ, Buhrmann R, Quigley HA, Johnson GJ. The definition and classification of glaucoma in prevalence surveys. *Br J Ophthalmol*. 2002;86(2):238-242. Medline:11815354 doi:10.1136/bjo.86.2.238

4. Zebardast N, Kavitha S, Krishnamurthy P, et al. Changes in anterior segment morphology and predictors of angle widening after laser iridotomy in South Indian eyes. *Ophthalmology*. 2016;123(12):2519-2526. Medline:27726963 doi:10.1016/j.ophtha.2016.08.020

5. Baskaran M, Kumar RS, Friedman DS, et al. The Singapore Asymptomatic Narrow Angles Laser Iridotomy Study: five-year results of a randomized controlled trial. *Ophthalmology*. 2022;129(2):147-158. Medline:34453952 doi:10.1016/j.ophtha.2021.08.017

6. He M, Jiang Y, Huang S, et al. Laser peripheral iridotomy for the prevention of angle closure: a single-centre, randomised controlled trial. *Lancet*. 2019;393(10181):1609-1618. Medline:30878226 doi:10.1016/S0140-6736(18)32607-2

7. Liao C, Quigley H, Jiang Y, et al. Iris volume change with physiologic mydriasis to identify development of angle closure: the Zhongshan Angle Closure Prevention Trial. *Br J Ophthalmol*. 2023;bjo-2022-322981. Medline:37236768 doi:10.1136/bjo-2022-322981

8. Xu BY, Friedman DS, Foster PJ, et al. Ocular biometric risk factors for progression of primary angle closure disease: the Zhongshan Angle Closure Prevention Trial. *Ophthalmology*. 2022;129(3):267-275. Medline:34634364 doi:10.1016/j.ophtha.2021.10.003

9. Liang Y, Friedman DS, Zhou Q, et al; Handan Eye Study Group. Prevalence and characteristics of primary angle-closure diseases in a rural adult Chinese population: the Handan Eye Study. *Invest Ophthalmol Vis Sci*. 2011;52(12):8672-8679. Medline:21908580 doi:10.1167/iovs.11-7480

10. Yamamoto T, Iwase A, Araie M, et al; Tajimi Study Group, Japan Glaucoma Society. The Tajimi Study report 2: prevalence of primary angle closure and secondary glaucoma in a Japanese population. *Ophthalmology*. 2005;112(10):1661-1669. Medline:16111758 doi:10.1016/j.ophtha.2005.05.012

11. Yuan Y, Wang W, Xiong R, et al. Fourteen-year outcome of angle-closure prevention with laser iridotomy in the Zhongshan Angle-Closure Prevention Study: extended follow-up of a randomized controlled trial. *Ophthalmology*. 2023;130(8):786-794. Medline:37030454 doi:10.1016/j.ophtha.2023.03.024

12. Jiang Y, Friedman DS, He M, Huang S, Kong X, Foster PJ. Design and methodology of a randomized controlled trial of laser iridotomy for the prevention of angle closure in southern China: the Zhongshan Angle Closure Prevention trial. *Ophthalmic Epidemiol*. 2010;17(5):321-332. Medline:20868259 doi:10.3109/09286586.2010.508353

13. World Medical Association. World Medical Association Declaration of Helsinki: ethical principles for medical research involving human subjects. *JAMA*. 2013;310(20):2191-2194. Medline:24141714 doi:10.1001/jama.2013.281053

14. von Elm E, Altman DG, Egger M, Pocock SJ, Gøtzsche PC, Vandenbroucke JP; STROBE Initiative. The Strengthening the Reporting of Observational Studies in Epidemiology (STROBE) statement: guidelines for reporting observational studies. *Lancet*. 2007;370(9596):1453-1457. Medline:18064739 doi:10.1016/S0140-6736(07)61602-X

15. Van Herick W, Shaffer RN, Schwartz A. Estimation of width of angle of anterior chamber. Incidence and significance of the narrow angle. *Am J Ophthalmol*. 1969;68(4):626-629. Medline:5344324 doi:10.1016/0002-9394(69)91241-0

16. Console JW, Sakata LM, Aung T, Friedman DS, He M. Quantitative analysis of anterior segment optical coherence tomography images: the Zhongshan Angle

Assessment Program. *Br J Ophthalmol*. 2008;92(12):1612-1616. Medline:18617543 doi:10.1136/bjo.2007.129932

17. Teo ZL, Soh ZD, Tham YC, et al. Six-year incidence and risk factors for primary angle-closure disease: the Singapore Epidemiology of Eye Diseases study. *Ophthalmology*. 2022;129(7):792-802. Medline:35306094 doi:10.1016/j.ophtha.2022.03.009

18. Xu BY, Lifton J, Burkemper B, et al. ocular biometric determinants of anterior chamber angle width in Chinese Americans: the Chinese American Eye Study. *Am J Ophthalmol*. 2020;220:19-26. Medline:32730913 doi:10.1016/j.ajo.2020.07.030

19. Wang L, Huang W, Huang S, et al. Ten-year incidence of primary angle closure in elderly Chinese: the Liwan Eye Study. *Br J Ophthalmol*. 2019;103(3):355-360. Medline:29777045 doi:10.1136/bjophthalmol-2017-311808

20. Zhang Y, Zhang Q, Thomas R, Li SZ, Wang NL. Development of angle closure and associated risk factors: the Handan Eye Study. *Acta Ophthalmol*. 2022;100(1):e253-e261. Medline:33960669 doi:10.1111/aos.14887

21. Jindal A, Ctori I, Virgili G, Lucenteforte E, Lawrenson JG. Non-contact tests for identifying people at risk of primary angle closure glaucoma. *Cochrane Database Syst Rev*. 2020;5(5):CD012947. Medline:32468576

22. Halawa OA, Zebardast N, Kolli A, et al. Population-based utility of van Herick grading for angle-closure detection. *Ophthalmology*. 2021;128(12):1779-1782. Medline:34129876 doi:10.1016/j.ophtha.2021.06.010

23. Su DHW, Friedman DS, See JLS, et al. Degree of angle closure and extent of peripheral anterior synechiae: an anterior segment OCT study. *Br J Ophthalmol*. 2008;92(1):103-107. Medline:17584995 doi:10.1136/bjo.2007.122572

24. Xu BY, Liang S, Pardeshi AA, et al. Differences in ocular biometric measurements among subtypes of primary angle closure disease: the Chinese American Eye Study. *Ophthalmol Glaucoma*. 2021;4(2):224-231. Medline:32942063 doi:10.1016/j.ogla.2020.09.008

25. Jiang Y, Wang W, Wang L, He M. Association of anterior segment parameters and 5-year incident narrow angles: findings from an older Chinese population. *Br J*

Ophthalmol. 2021;105(7):970-976. Medline:32699050 doi:10.1136/bjophthalmol-2020-315852

26. Nongpiur ME, Aboobakar IF, Baskaran M, et al. Association of baseline anterior segment parameters with the development of incident gonioscopic angle closure. *JAMA Ophthalmol.* 2017;135(3):252-258. Medline:28196218 doi:10.1001/jamaophthalmol.2016.5847

27. Dai Y, Zhang S, Shen M, et al. Identification of peripheral anterior synechia with anterior segment optical coherence tomography. *Graefes Arch Clin Exp Ophthalmol.* 2021;259(9):2753-2759. Medline:33974133 doi:10.1007/s00417-021-05220-1

28. Mishima K, Tomidokoro A, Suramethakul P, et al. Iridotrabecular contact observed using anterior segment three-dimensional OCT in eyes with a shallow peripheral anterior chamber. *Invest Ophthalmol Vis Sci.* 2013;54(7):4628-4635. Medline:23761081 doi:10.1167/iovs.12-11230

29. Leung CK, Cheung CY, Li H, et al. Dynamic analysis of dark-light changes of the anterior chamber angle with anterior segment OCT. *Invest Ophthalmol Vis Sci.* 2007;48(9):4116-4122. Medline:17724195 doi:10.1167/iovs.07-0010

30. Nolan WP, See JL, Chew PT, et al. Detection of primary angle closure using anterior segment optical coherence tomography in Asian eyes. *Ophthalmology.* 2007;114(1):33-39. Medline:17070597 doi:10.1016/j.ophtha.2006.05.073

31. Zheng C, Cheung CY, Narayanaswamy A, et al. Pupil dynamics in Chinese subjects with angle closure. *Graefes Arch Clin Exp Ophthalmol.* 2012;250(9):1353-1359. Medline:22290071 doi:10.1007/s00417-012-1934-7

32. Quigley HA. Angle-closure glaucoma—simpler answers to complex mechanisms: LXVI Edward Jackson Memorial Lecture. *Am J Ophthalmol.* 2009;148(5):657-669.e1. Medline:19878757 doi:10.1016/j.ajo.2009.08.009

33. Wanichwecharungruang B, Pattanapongpaiboon W, Kongsomboon K, Parivisutt N, Annopawong K, Seresirikachorn K. Diagnostic performance of anterior segment optical coherence tomography in detecting plateau iris. *BMJ Open Ophthalmol.* 2022;7(1):e000931. Medline:35402728 doi:10.1136/bmjophth-2021-000931

Table 1. Baseline Characteristics of Untreated PACS Eyes Stratified According to Progression to PAC During 14 Years of Follow-Up

Characteristic	Progression from PACS to PAC, mean (SD)		Difference (95% CI)
	Yes (n = 93)	No (n = 284)	
Demographics			
Age, y	58.73 (4.94)	58.13 (4.63)	−0.59 (−1.70 to 0.51)
Sex, No. (%)			
Female	80 (86%)	237 (83%)	−3% (−11% to 6%)
Male	13 (14%)	47 (17%)	3% (−6% to 11%)
Total angle width score [a]	4.94 (2.63)	5.53 (2.24)	0.60 (0.05 to 1.15)
Limbal ACD, PCT	0.20 (0.08)	0.23 (0.07)	0.03 (0.01 to 0.04)
IOP, mm Hg	15.67 (2.86)	14.73 (2.76)	−0.93 (−1.59 to −0.28)
Change in IOP after DRPPT, mm Hg [b]	4.48 (2.95)	4.43 (2.98)	−0.05 (−0.75 to 0.65)
Axial length, mm	22.50 (0.74)	22.50 (0.74)	0 (−0.17 to 0.18)
Central ACD, mm	2.50 (0.21)	2.60 (0.20)	0.10 (0.05 to 0.15)
Lens thickness, mm	4.90 (0.33)	4.82 (0.27)	−0.08 (−0.15 to −0.01)
Light-room AS-OCT metric			
ACW, mm	11.38 (0.39)	11.42 (0.36)	0.04 (−0.04 to 0.13)
ACA, mm^2	14.60 (1.94)	15.35 (1.93)	0.75 (0.29 to 1.20)
LV, mm	0.78 (0.17)	0.74 (0.18)	−0.04 (−0.08 to 0.01)
PD, mm	2.69 (0.51)	2.73 (0.52)	0.04 (−0.08 to 0.16)
AOD at 500 μm, mm	0.14 (0.06)	0.17 (0.06)	0.02 (0.01 to 0.04)
TISA at 500 μm, mm^2	0.07 (0.03)	0.08 (0.02)	0.01 (0 to 0.02)
ARA at 750 μm, mm^2	0.14 (0.05)	0.17 (0.06)	0.02 (0.01 to 0.04)
IT at 750 μm, mm	0.44 (0.09)	0.46 (0.08)	0.02 (−0.01 to 0.04)
IAREA, mm^2	1.89 (0.26)	1.90 (0.27)	0.01 (−0.05 to 0.07)
ICURV, mm	0.43 (0.11)	0.43 (0.11)	0 (−0.02 to 0.03)
Dark-room AS-OCT metric			
ACW, mm	11.36 (0.37)	11.41 (0.37)	0.06 (−0.03 to 0.14)
ACA, mm^2	15.31 (1.99)	16.02 (1.98)	0.72 (0.25 to 1.18)
LV, mm	0.75 (0.18)	0.73 (0.18)	−0.03 (−0.07 to 0.01)
PD, mm	4.41 (0.73)	4.45 (0.69)	0.04 (−0.12 to 0.21)
AOD at 500 μm, mm	0.08 (0.05)	0.09 (0.06)	0.02 (0 to 0.03)
TISA at 500 μm, mm^2	0.04 (0.03)	0.05 (0.03)	0.01 (0 to 0.02)

ARA at 750 μm, mm²	0.09 (0.05)	0.11 (0.06)	0.02 (0.01 to 0.03)
IT at 750 μm, mm	0.49 (0.09)	0.50 (0.09)	0.01 (−0.01 to 0.03)
IAREA, mm²	1.55 (0.18)	1.56 (0.22)	0.01 (−0.04 to 0.06)
ICURV, mm	0.43 (0.10)	0.44 (0.10)	0.01 (−0.02 to 0.03)
Change in AS-OCT metric from light to dark [c]			
ACW, mm	0.02 (0.14)	0.01 (0.14)	−0.01 (−0.05 to 0.02)
ACA, mm²	−0.70 (0.32)	−0.67 (0.36)	0.03 (−0.05 to 0.11)
LV, mm	0.03 (0.07)	0.02 (0.08)	−0.01 (−0.03 to 0.01)
PD, mm	−1.72 (0.68)	−1.72 (0.63)	0 (−0.15 to 0.15)
AOD at 500 μm, mm	0.07 (0.04)	0.07 (0.05)	0.01 (−0.01 to 0.02)
TISA at 500 μm, mm²	0.03 (0.02)	0.03 (0.02)	0 (0 to 0.01)
ARA at 750 μm, mm²	0.05 (0.04)	0.06 (0.05)	0.01 (0 to 0.02)
IT at 750 μm, mm	−0.05 (0.09)	−0.04 (0.08)	0.01 (−0.01 to 0.03)
IAREA, mm²	0.33 (0.15)	0.33 (0.17)	0 (−0.04 to 0.04)
ICURV, mm	0 (0.09)	0 (0.09)	0 (−0.02 to 0.02)

Abbreviations: ACA, anterior chamber area; ACD, anterior chamber depth; ACW, anterior chamber width; AOD, angle opening distance; ARA, angle recess area; AS-OCT, anterior segment optical coherence tomography; DRPPT, dark room prone provocative test; IAREA, iris area; ICURV, iris curvature; IOP, intraocular pressure; IT, iris thickness; LV, lens vault; PAC, primary angle closure; PACS, PAC suspect; PCT, peripheral corneal thickness; PD, pupil diameter; TISA, trabecular iris space area.

[a]Calculated by summing the Shaffer grading of all 4 quadrants (0-16, with higher points representing larger angle width).

[b]Calculated by subtracting measures before the test from measures after the test.

[c]Calculated by subtracting dark-room values from corresponding light-room values.

Table 2. Logistic Regression Models of the Risk of Progression From Primary Angle Closure Suspect to Primary Angle Closure During 14 Years of Follow-Up Based on Light-Room Anterior Segment Optical Coherence Tomography

Covariate at baseline	Univariable model		Multivariable model A [a]	
	OR (95% CI)	P value	OR (95% CI)	P value
Age, per 1-y increase	1.03 (0.98-1.08)	.29	NA	NA
Female vs male	1.22 (0.63-2.37)	.56	NA	NA
Total angle width score, per 1-point increase	0.90 (0.81-0.99)	.04	0.98 (0.87-1.09)	.68
Limbal ACD, per 0.01-PCT increase	0.94 (0.91-0.98)	.002	0.96 (0.93-0.99)	.04
IOP, per 1-mm Hg increase	1.13 (1.04-1.23)	.006	1.14 (1.04-1.25)	.004
Change in IOP after DRPPT, per 1-mm Hg increase [b]	1.01 (0.93-1.09)	.89	NA	NA
Axial length, per 1-mm increase	0.99 (0.72-1.36)	.96	NA	NA
Central ACD, per 0.1-mm increase	0.80 (0.71-0.90)	<.001	0.81 (0.67-0.97)	.02
Lens thickness, per 0.1-mm increase	1.11 (1.02-1.20)	.02	1.05 (0.95-1.16)	.38
Light-room ACW, per 0.1-mm increase	0.97 (0.91-1.03)	.33	NA	NA
Light-room ACA, per 0.1-mm^2 increase	0.98 (0.97-0.99)	.002	1.00 (0.98-1.02)	.83
Light-room LV, per 0.1-mm increase	1.13 (0.99-1.29)	.08	0.92 (0.77-1.09)	.34
Light-room PD, per 0.1-mm increase	0.99 (0.94-1.03)	.53	NA	NA
Light-room AOD at 500 μm, per 0.01-mm increase	0.93 (0.89-0.97)	.001	0.96 (0.91-1.01)	.09
Light-room TISA at 500 μm, per 0.01-mm^2 increase	0.82 (0.74-0.91)	<.001	NA	NA

Light-room ARA at 750 μm, per 0.01-mm^2 increase	0.91 (0.87-0.96)	<.001	NA	NA
Light-room IT at 750 μm, per 0.1-mm increase	0.80 (0.60-1.06)	.13	NA	NA
Light-room IAREA, per 0.1-mm^2 increase	0.99 (0.90-1.08)	.75	NA	NA
Light-room ICURV, per 0.1-mm increase	0.96 (0.77-1.19)	.70	NA	NA

Abbreviations: ACA, anterior chamber area; ACD, anterior chamber depth; ACW, anterior chamber width; AOD, angle opening distance; ARA, angle recess area; DRPPT, dark room prone provocative test; IAREA, iris area; ICURV, iris curvature; IOP, intraocular pressure; IT, iris thickness; NA, not applicable; LV, lens vault; OR, odds ratio; PCT, peripheral corneal thickness; PD, pupil diameter; TISA, trabecular iris space area.

[a] Model A was adjusted for baseline covariates with a P value <0.10 in univariable models and included light-room AOD at 500 μm.

[b] Calculated by subtracting measures before the test from measures after the test.

Table 3. Multivariable Logistic Regression Models of the Progression From Primary Angle Closure Suspect to Primary Angle Closure During 14 Years of Follow-Up

Covariate at baseline	Multivariable model B [a]		Multivariable model C [b]	
	OR (95% CI)	P value	OR (95% CI)	P value
Total angle width score, per 1-point increase	0.98 (0.88-1.10)	.74	0.98 (0.88-1.10)	.78
Limbal ACD, per 0.01-PCT increase	0.97 (0.93-1.00)	.08	0.97 (0.93-1.00)	.08
IOP, per 1-mm Hg increase	1.14 (1.04-1.25)	.005	1.15 (1.05-1.26)	.004
Central ACD, per 0.1-mm increase	0.80 (0.67-0.96)	.02	0.80 (0.66-0.96)	.02
Lens thickness, per 0.1-mm increase	1.04 (0.94-1.16)	.44	1.05 (0.95-1.16)	.37
Light-room				
AS-OCT parameters				
ACA, per 0.1-mm^2 increase	1.00 (0.98-1.02)	.89	1.00 (0.98-1.02)	.87
LV, per 0.1-mm increase	0.93 (0.78-1.11)	.42	0.92 (0.77-1.09)	.33
TISA at 500 μm, per 0.01-mm^2 increase	0.86 (0.77-0.96)	.006	NA	NA
ARA at 750 μm, per 0.01-mm^2 increase	NA	NA	0.93 (0.88-0.98)	.008

Abbreviations: ACA, anterior chamber area; ACD, anterior chamber depth; ARA, angle recess area; AS-OCT, anterior segment optical coherence tomography; IOP, intraocular pressure; NA, not applicable; LV, lens vault; OR, odds ratio; PCT, peripheral corneal thickness; TISA, trabecular iris space area.

[a] In model B, light-room angle opening distance at 500 μm in multivariable model A is replaced by light-room TISA at 500 μm.

[b] In model C, light-room angle opening distance at 500 μm in multivariable model A is replaced by light-room ARA at 750 μm.

Table 4. Models' Performance for Predicting the 14-Year Risk of Progression From Primary Angle Closure Suspect to Primary Angle Closure

Covariate at baseline	OR (95% CI)			
	Prediction model A [a]	Prediction model B [b]	Prediction model C [c]	Prediction model D [d]
IOP, per 1-mm Hg increase	1.15 (1.06-1.26)	1.15 (1.05-1.26)	1.15 (1.05-1.26)	1.14 (1.05-1.25)
Central ACD, per 0.1-mm increase	0.80 (0.70-0.90)	0.80 (0.70-0.90)	0.80 (0.70-0.90)	0.78 (0.69-0.89)
Limbal ACD, per 0.01-PCT increase	0.96 (0.92-0.99)	NA	NA	NA
Light-room TISA at 500 μm, per 0.01-mm² increase	NA	0.84 (0.76-0.93)	NA	NA
Light-room ARA at 750 μm, per 0.01-mm² increase	NA	NA	0.92 (0.88-0.97)	NA
Dark-room TISA at 500 μm, per 0.01-mm² increase	NA	NA	NA	0.87 (0.79-0.95)
Model performance, estimates (95% CI)				
Sensitivity	0.59 (0.48-0.69)	0.69 (0.58-0.78)	0.66 (0.55-0.75)	0.57 (0.46-0.67)
Specificity	0.73 (0.68-0.78)	0.64 (0.58-0.69)	0.67 (0.61-0.73)	0.74 (0.68-0.79)
PPV	0.42 (0.33-0.51)	0.38 (0.31-0.46)	0.40 (0.32-0.48)	0.42 (0.33-0.51)
NPV	0.85 (0.79-0.89)	0.86 (0.81-0.91)	0.86 (0.80-0.90)	0.84 (0.79-0.88)
AUROC	0.69 (0.63-0.75)	0.70 (0.64-0.76)	0.70 (0.64-0.76)	0.69 (0.62-0.75)

Abbreviations: ACD, anterior chamber depth; ARA, angle recess area; AUROC, area under the receiver operating characteristic curve; IOP, intraocular pressure; NA, not applicable; NPV, negative predictive value; OR, odds ratio; PCT, peripheral corneal thickness; PPV, positive predictive value; TISA, trabecular iris space area.

[a] Prediction model A included IOP and central and limbal ACDs.

[b] Prediction model B included IOP, central ACD, and light-room TISA at 500 μm.

[c] Prediction model C included IOP, central ACD, and light-room ARA at 750 μm.

[d] Prediction model D included IOP, central ACD, and dark-room TISA at 500 μm.

Supplemental Online Content

eTable 1. Baseline Characteristics Between Eyes Included and Not Included in the Analysis

Covariates	Mean (SD) or Number (%)		Difference (95% CI)
	Included eyes (n=377)	Excluded eyes (n=512)	
Age (year)	58.28 (4.71)	60.12 (5.12)	1.84 (1.18 to 2.50)
Sex, No. (%)			
Female	317 (84%)	420 (82%)	-2% (-7% to 3%)
Male	60 (16%)	92 (18%)	2% (-3% to 7%)
IOP (mmHg)	14.96 (2.81)	15.19 (2.84)	0.23 (-0.15 to 0.60)
Total angle width (point) [a]	5.38 (2.35)	5.31 (2.44)	-0.07 (-0.39 to 0.25)
Limbal ACD (PCT)	0.22 (0.07)	0.22 (0.08)	0 (-0.02 to 0.01)
Change in IOP after DRPPT (mmHg) [b]	4.45 (2.97)	4.04 (2.94)	-0.40 (-0.79 to -0.01)
Axial length (mm)	22.50 (0.74)	22.48 (0.71)	-0.02 (-0.12 to 0.08)
Central ACD (mm)	2.57 (0.21)	2.53 (0.23)	-0.04 (-0.07 to -0.01)
Lens thickness (mm)	4.84 (0.29)	4.91 (0.33)	0.07 (0.03 to 0.11)

[a] Calculated by summing the Shaffer grading of all 4 quadrants (0-16, with higher points representing larger angle width);

[b] Calculated by subtracting measures before the test from measures after the test; SD= Standard deviation; 95%CI= 95% confidence interval; IOP = Intraocular pressure; ACD = Anterior chamber depth; PCT= Peripheral corneal thickness; DRPPT = Dark room prone provocative test.

eTable 2. Clinical Characteristics of Eyes With Primary Angle Closure at Diagnosis

Characteristics	Number (n=93)
Events	
PAS	88 (95%)
IOP>24 mmHg [a]	6 (7%)
AAC	3 (3%)
Diagnosed at which visit	
0.5-3 years	14 (15%)
4.5-6 years	15 (16%)
14 years	64 (69%)
Total angle width at diagnosis	
0 point	58 (62%)
1-2 points	23 (25%)
≥3 points	12 (13%)
IOP at diagnosis	
≤14 mmHg	26 (28%)
15-20 mmHg	54 (58%)
≥21 mmHg	13 (14%)
PAS range at diagnosis	
0 o'clock	5 (5%)
1 o'clock	61 (66%)
≥2 o'clock	27 (29%)
PAS location at diagnosis [b]	
Superior	68 (73%)
Nasal and Temporal	24 (26%)
Inferior	10 (11%)

[a] Three eyes had PAS together with IOP >24mmHg at diagnosis; one eye had PAS together with AAC at diagnosis;

[b] Seven eyes had PAS in superior and nasal quadrants; One eye had PAS in superior and inferior quadrants; One eye had PAS in superior and temporal quadrants; Two eyes had PAS in nasal and inferior quadrants; One eye had PAS in inferior and temporal quadrants; One eye had PAS in superior, nasal and inferior quadrants.

PAS= Peripheral angle synechiae; IOP= Intraocular pressure; AAC= Acute angle closure

eTable 3. Logistic Regression Models of the Progression From PACS to PAC During 14 Years of Follow-Up Based on Dark-Room AS-OCT

Covariates at baseline	Uni-variate model		Multi-variate model D	
	OR (95%CI)	P value	OR (95%CI)	P value
Age, per 1-year increase	1.03 (0.98 to 1.08)	.29	-	-
Female vs. Male	1.22 (0.63 to 2.37)	.56	-	-
Total angle width score, per 1-point increase	0.90 (0.81 to 0.99)	.04	0.99 (0.88 to 1.10)	.82
Limbal ACD, per 0.01-PCT increase	0.94 (0.91 to 0.98)	.002	0.97 (0.93 to 1.00)	.07
IOP, per 1-mm Hg increase	1.13 (1.04 to 1.23)	.006	1.14 (1.04 to 1.25)	.005
Δ IOP after DRPPT, per 1-mm Hg increase [a]	1.01 (0.93 to 1.09)	.89	-	-
Axial length, per 1-mm increase	0.99 (0.72 to 1.36)	.96	-	-
Central ACD, per 0.1-mm increase	0.80 (0.71 to 0.90)	<.001	0.81 (0.67 to 0.97)	.02
Lens thickness, per 0.1-mm increase	1.11 (1.02 to 1.20)	.02	1.03 (0.94 to 1.14)	.50
Dark-room AS-OCT				
Dark-room anterior chamber width, per 0.1-mm increase	0.96 (0.90 to 1.02)	.20	-	-
Dark-room anterior chamber area, per 0.1-mm^2 increase	0.98 (0.97 to 0.99)	.003	1.00 (0.98 to 1.02)	.87
Dark-room LV, per 0.1-mm increase	1.09 (0.96 to 1.25)	.19	-	-
Dark-room PD, per 0.1-mm increase	0.99 (0.96 to 1.03)	.62	-	-
Dark-room AOD at 500 μm, per 0.01-mm increase	0.95 (0.91 to 0.99)	.01		
Dark-room TISA at 500 μm, per 0.01-mm^2 increase	0.86 (0.78 to 0.94)	.001	0.89 (0.80 to 0.98)	.02

Dark-room ARA at 750 μm, per 0.01-mm² increase	0.93 (0.89 to 0.98)	.004	-	-
Dark-room IT at 750 μm, per 0.1-mm increase	0.92 (0.70 to 1.20)	.53	-	-
Dark-room IAREA, per 0.1-mm² increase	0.98 (0.87 to 1.09)	.67	-	-
Dark-room ICURV, per 0.1-mm increase	0.94 (0.74 to 1.19)	.59	-	-

[a] Calculated by subtracting measures before the test from measures after the test; PACS= Primary angle closure suspect; PAC= Primary angle closure; AS-OCT= Anterior segment optical coherence tomography; OR= Odds ratio; 95% CI= 95% confidence interval; ACD= Anterior chamber depth; PCT= Peripheral corneal thickness; IOP=Intraocular pressure; DRPPT= Dark room prone provocative test; LV= Lens vault; PD= Pupil diameter; AOD= Angle opening distance; TISA= Trabecular iris space area; ARA= Angle recess area; IT= Iris thickness; IAREA= Iris area; ICURV= Iris curvature.

eTable 4. Multivariable Logistic Regression Models of the Progression From PACS to PAC During 14 Years of Follow-Up With Dark-Room TISA at 500 μm Replaced by Dark-Room AOD at 500 μm and Dark-Room ARA at 750 μm

Covariates at baseline	Multi-variate model E		Multi-variate model F	
	OR (95%CI)	P value	OR (95%CI)	P value
Total angle width score, per 1-point increase	0.97 (0.87 to 1.09)	.63	0.98 (0.88 to 1.10)	.75
Limbal ACD, per 0.01-PCT increase	0.96 (0.93 to 0.99)	.04	0.96 (0.93 to 1.00)	.07
IOP, per 1-mm Hg increase	1.15 (1.05 to 1.26)	.003	1.14 (1.04 to 1.25)	.004
Central ACD, per 0.1-mm increase	0.81 (0.68 to 0.97)	.02	0.81 (0.67 to 0.97)	.02
Lens thickness, per 0.1-mm increase	1.04 (0.94 to 1.14)	.47	1.04 (0.94 to 1.14)	.48
Dark-room AS-OCT				
Dark-room anterior chamber area, per 0.1-mm^2 increase	1.00 (0.99 to 1.02)	.76	1.00 (0.98 to 1.02)	.77
Dark-room AOD at 500 μm, per 0.01-mm increase	0.98 (0.93 to 1.03)	.33	-	-
Dark-room ARA at 750 μm, per 0.01-mm^2 increase	-	-	0.96 (0.91 to 1.01)	.10

PACS= Primary angle closure suspect; PAC= Primary angle closure; OR= Odds ratio; 95% CI= 95% confidence interval; PCT= Peripheral corneal thickness; ACD= Anterior chamber depth; ACA= Anterior chamber area; AOD= Angle opening distance; ARA= Angle recess area.

eTable 5. Multivariable Logistic Regression Models of the Progression From PACS to PAC During 14 Years of Follow-Up With Light-to-Dark Changes of AS-OCT Metrics Compulsively Included

Covariates at baseline	Model A + Dynamic metrics *		Model B + Dynamic metrics *		Model C + Dynamic metrics *	
	OR (95%CI)	P value	OR (95%CI)	P value	OR (95%CI)	P value
Total angle width score, per 1-point increase	0.99 (0.88 to 1.11)	.81	0.99 (0.88 to 1.11)	.86	0.99 (0.88 to 1.11)	.85
Limbal ACD, per 0.01-PCT increase	0.96 (0.93 to 1.00)	.06	0.97 (0.93 to 1.01)	.10	0.97 (0.93 to 1.01)	.09
IOP, per 1-mm Hg increase	1.15 (1.04 to 1.26)	.004	1.15 (1.05 to 1.26)	.004	1.15 (1.05 to 1.27)	.003
Central ACD, per 0.1-mm increase	0.80 (0.66 to 0.97)	.02	0.79 (0.65 to 0.96)	.02	0.79 (0.65 to 0.96)	.02
Lens thickness, per 0.1-mm increase	1.06 (0.95 to 1.18)	.30	1.05 (0.95 to 1.17)	.34	1.06 (0.95 to 1.19)	.26
Light-room AS-OCT metrics						
Light-room anterior chamber area, per 0.1- mm² increase	1.00 (0.98 to 1.02)	.90	1.00 (0.98 to 1.02)	.95	1.00 (0.98 to 1.02)	.98
Light-room LV, per 0.1-mm increase	0.90 (0.75 to 1.08)	.25	0.91 (0.76 to 1.10)	.35	0.90 (0.75 to 1.08)	.24
Light-room AOD at 500 μm, per 0.01-mm increase	0.95 (0.90 to 1.01)	.11	-	-	-	-
Light-room TISA at 500 μm, per 0.01-mm² increase	-	-	0.84 (0.75 to 0.95)	.005	-	-
Light-room ARA at 750 μm, per 0.01-mm² increase	-	-	-	-	0.93 (0.88 to 0.99)	.03
Changes in AS-OCT metrics from light to dark [a]						
Δ Anterior chamber width, per 0.1-mm increase	1.00 (0.73 to 1.37)	.99	1.03 (0.75 to 1.40)	.87	0.98 (0.71 to 1.35)	.91

Δ Anterior chamber area, per 0.1-mm² increase	0.99 (0.90 to 1.09)	.82	0.99 (0.90 to 1.09)	.81	1.01 (0.92 to 1.12)	.82
Δ LV, per 0.01-mm increase	1.01 (0.96 to 1.07)	.61	1.01 (0.96 to 1.07)	.70	1.01 (0.96 to 1.07)	.62
Δ PD, per 0.1-mm increase	0.99 (0.92 to 1.06)	.69	0.99 (0.92 to 1.06)	.75	0.98 (0.92 to 1.05)	.62
Δ AOD at 500 μm, per 0.01-mm increase	0.98 (0.91 to 1.06)	.68	-	-	-	-
Δ TISA at 500 μm, per 0.01-mm² increase	-	-	0.99 (0.81 to 1.20)	.90	-	-
Δ ARA at 750 μm, per 0.01-mm² increase	-	-	-	-	0.98 (0.90 to 1.06)	.59
Δ IT at 750 μm, per 0.01-mm increase	1.00 (0.95 to 1.04)	.84	1.00 (0.96 to 1.05)	.89	0.99 (0.95 to 1.04)	.79
Δ IAREA, per 0.01-mm² increase	1.00 (0.98 to 1.03)	.80	1.00 (0.98 to 1.03)	.75	1.01 (0.98 to 1.04)	.66
Δ ICURV, per 0.01-mm increase	0.99 (0.96 to 1.02)	.42	0.98 (0.95 to 1.02)	.33	0.99 (0.96 to 1.02)	.49

[a] Calculated by subtracting dark-room values from corresponding light-room values.

PACS = Primary angle closure suspect; PAC = Primary angle closure; OR = Odds ratio; 95% CI = 95% confidence interval; AS-OCT = Anterior segment optical coherence tomography; ACD = Anterior chamber depth; PCT= Peripheral corneal thickness; DRPPT = Dark room prone provocative test; LV = Lens vault; PD = Pupil diameter; AOD = Angle opening distance; TISA = Trabecular iris space area; ARA = Angle recess area; IT = Iris thickness; IAREA = Iris area; ICURV = Iris curvature.

eTable 6. Cumulative Incidence Rate and 95% CIs of Progression From PACS to PAC During 14 Years of Follow-Up in Risk Levels Estimated by IOP, Central ACD, Limbal ACD, and Prediction Model A

	Risk of progression based on the Prediction model A			
	< 20%	20% to 30%	>30%	Total
Total	23 / 158 (0.15)	20 / 104 (0.19)	50 / 115 (0.43)	93 / 377 (0.25)
	[0.09 to 0.21]	[0.12 to 0.28]	[0.34 to 0.53]	[0.20 to 0.29]
Risk of progression based on IOP				
< 20%	6 / 63 (0.10)	2 / 10 (0.20)	2 / 7 (0.29)	10 / 80 (0.13)
(<13 mmHg)	[0.04 to 0.20]	[0.03 to 0.56]	[0.04 to 0.71]	[0.06 to 0.22]
20% to 30%	16 / 89 (0.18)	16 / 73 (0.22)	27 / 67 (0.40)	59 / 229 (0.26)
(13 to 17 mmHg)	[0.11 to 0.28]	[0.13 to 0.33]	[0.28 to 0.53]	[0.20 to 0.32]
>30%	1 / 6 (0.17)	2 / 21 (0.10)	21 / 41 (0.51)	24 / 68 (0.35)
(>17 mmHg)	[0.01 to 0.64]	[0.01 to 0.30]	[0.35 to 0.67]	[0.24 to 0.48]
Risk of progression based on central ACD				
< 20%	13 / 98 (0.13)	2 / 17 (0.12)	2 / 4 (0.50)	17 / 119 (0.14)
(>2.66 mm)	[0.07 to 0.22]	[0.01 to 0.36]	[0.07 to 0.93]	[0.09 to 0.22]
20% to 30%	9 / 52 (0.17)	12 / 66 (0.18)	21 / 44 (0.48)	42 / 162 (0.26)
(2.43 to 2.66 mm)	[0.08 to 0.30]	[0.10 to 0.30]	[0.32 to 0.63]	[0.19 to 0.33]
>30%	1 / 8 (0.13)	6 / 21 (0.29)	27 / 67 (0.40)	34 / 96 (0.35)
(<2.43 mm)	[0.01 to 0.53]	[0.11 to 0.52]	[0.28 to 0.53]	[0.26 to 0.46]
Risk of progression based on limbal ACD				
< 20%	4 / 18 (0.22)	1 / 3 (0.33)	1 / 1 (1.00)	6 / 22 (0.27)
(>0.25 PCT)	[0.06 to 0.48]	[0.01 to 0.91]	[0.03 to 1.00] [a]	[0.11 to 0.50]
20% to 30%	15 / 126 (0.12)	13 / 69 (0.19)	16 / 39 (0.41)	44 / 234 (0.19)
(0.25 PCT)	[0.07 to 0.19]	[0.10 to 0.30]	[0.26 to 0.58]	[0.14 to 0.24]
>30%	4 / 14 (0.29)	6 / 32 (0.19)	33 / 75 (0.44)	43 / 121 (0.36)
(<0.25 PCT)	[0.08 to 0.58]	[0.07 to 0.36]	[0.33 to 0.56]	[0.27 to 0.45]

Data are presented as "Progression/ Total (Incidence) [95% confidence interval]"

[a] One-sided, 97.5% confidence interval was provided.

Prediction model A includes IOP, both central and limbal ACDs.

PACS= Primary angle closure suspect; PAC= Primary angle closure; IOP=Intraocular pressure; ACD= Anterior chamber depth; PCT= Peripheral corneal thickness.

eTable 7. Cumulative Incidence Rate and 95% CIs of Progression From PACS to PAC During 14 Years of Follow-Up in Risk Levels Estimated by IOP, Central ACD, Light-Room TISA at 500 μm, and Prediction Model B

	Risk of progression based on the Prediction model B			
	< 20%	20% to 30%	>30%	Total
Total	20 / 154 (0.13) [0.08 to 0.19]	27 / 114 (0.24) [0.16 to 0.33]	46 / 109 (0.42) [0.33 to 0.52]	93 / 377 (0.25) [0.20 to 0.29]
Risk of progression based on IOP				
< 20% (<13 mmHg)	4 / 57 (0.07) [0.02 to 0.17]	3 / 15 (0.20) [0.04 to 0.48]	3 / 8 (0.38) [0.09 to 0.76]	10 / 80 (0.13) [0.06 to 0.22]
20% to 30% (13 to 17 mmHg)	13 / 86 (0.15) [0.08 to 0.24]	21 / 82 (0.26) [0.17 to 0.36]	25 / 61 (0.41) [0.29 to 0.54]	59 / 229 (0.26) [0.20 to 0.32]
>30% (>17 mmHg)	3 / 11 (0.27) [0.06 to 0.61]	3 / 17 (0.18) [0.04 to 0.43]	18 / 40 (0.45) [0.29 to 0.62]	24 / 68 (0.35) [0.24 to 0.48]
Risk of progression based on central ACD				
< 20% (>2.66 mm)	11 / 93 (0.12) [0.06 to 0.20]	5 / 23 (0.22) [0.07 to 0.44]	1 / 3 (0.33) [0.01 to 0.91]	17 / 119 (0.14) [0.09 to 0.22]
20% to 30% (2.43 to 2.66 mm)	7 / 51 (0.14) [0.06 to 0.26]	15 / 62 (0.24) [0.14 to 0.37]	20 / 49 (0.41) [0.27 to 0.56]	42 / 162 (0.26) [0.19 to 0.33]
>30% (<2.43 mm)	2 / 10 (0.20) [0.03 to 0.56]	7 / 29 (0.24) [0.10 to 0.44]	25 / 57 (0.44) [0.31 to 0.58]	34 / 96 (0.35) [0.26 to 0.46]
Risk of progression based on light-room TISA at 500 μm				
< 20% (>0.08 mm^2)	11 / 98 (0.11) [0.06 to 0.19]	8 / 31 (0.26) [0.12 to 0.45]	1 / 9 (0.11) [0.01 to 0.48]	20 / 138 (0.14) [0.09 to 0.21]
20% to 30% (0.06 to 0.08 mm^2)	8 / 43 (0.19) [0.08 to 0.33]	12 / 55 (0.22) [0.12 to 0.35]	14 / 35 (0.40) [0.24 to 0.58]	34 / 133 (0.26) [0.18 to 0.34]
>30% (<0.06 mm^2)	1 / 13 (0.08) [0.01 to 0.36]	7 / 28 (0.25) [0.11 to 0.45]	31 / 65 (0.48) [0.35 to 0.60]	39 / 106 (0.37) [0.28 to 0.47]

Data are presented as "Progression/ Total (Incidence) [95% confidence interval]"

Prediction model B includes IOP, both central ACD and light-room TISA at 500 μm.

PACS= Primary angle closure suspect; PAC= Primary angle closure; IOP=Intraocular pressure; ACD= Anterior chamber depth; TISA= Trabecular iris space area.

eTable 8. Cumulative Incidence Rate and 95% CIs of Progression From PACS to PAC During 14 Years of Follow-Up in Risk Levels Estimated by IOP, Central ACD, Light-Room ARA at 750 μm, and Prediction Model C

	Risk of progression based on the Prediction model C			
	< 20%	20% to 40%	>40%	Total
Total	20 / 161 (0.12)	27 / 104 (0.26)	46 / 112 (0.41)	93 / 377 (0.25)
	[0.08 to 0.19]	[0.18 to 0.35]	[0.32 to 0.51]	[0.20 to 0.29]
Risk of progression based on IOP				
< 20%	4 / 57 (0.07)	3 / 15 (0.20)	3 / 8 (0.38)	10 / 80 (0.13)
(<13 mmHg)	[0.02 to 0.17]	[0.04 to 0.48]	[0.09 to 0.76]	[0.06 to 0.22]
20% to 30%	14 / 92 (0.15)	20 / 74 (0.27)	25 / 63 (0.40)	59 / 229 (0.26)
(13 to 17 mmHg)	[0.09 to 0.24]	[0.17 to 0.39]	[0.28 to 0.53]	[0.20 to 0.32]
>30%	2 / 12 (0.17)	4 / 15 (0.27)	18 / 41 (0.44)	24 / 68 (0.35)
(>17 mmHg)	[0.02 to 0.48]	[0.08 to 0.55]	[0.28 to 0.60]	[0.24 to 0.48]
Risk of progression based on central ACD				
< 20%	13 / 98 (0.13)	3 / 19 (0.16)	1 / 2 (0.50)	17 / 119 (0.14)
(>2.66 mm)	[0.07 to 0.22]	[0.03 to 0.40]	[0.01 to 0.99]	[0.09 to 0.22]
20% to 30%	5 / 50 (0.10)	17 / 60 (0.28)	20 / 52 (0.38)	42 / 162 (0.26)
(2.43 to 2.66 mm)	[0.03 to 0.22]	[0.17 to 0.41]	[0.25 to 0.53]	[0.19 to 0.33]
>30%	2 / 13 (0.15)	7 / 25 (0.28)	25 / 58 (0.43)	34 / 96 (0.35)
(<2.43 mm)	[0.02 to 0.45]	[0.12 to 0.49]	[0.30 to 0.57]	[0.26 to 0.46]
Risk of progression based on light-room ARA at 750 μm				
< 20%	8 / 90 (0.09)	9 / 23 (0.39)	1 / 5 (0.20)	18 / 118 (0.15)
(>0.18 mm^2)	[0.04 to 0.17]	[0.20 to 0.61]	[0.01 to 0.72]	[0.09 to 0.23]
20% to 40%	11 / 59 (0.19)	12 / 53 (0.23)	12 / 39 (0.31)	35 / 151 (0.23)
(0.12 to 0.18 mm^2)	[0.10 to 0.31]	[0.12 to 0.36]	[0.17 to 0.48]	[0.17 to 0.31]
>40%	1 / 12 (0.08)	6 / 28 (0.21)	33 / 68 (0.49)	40 / 108 (0.37)
(<0.12 mm^2)	[0.01 to 0.38]	[0.08 to 0.41]	[0.36 to 0.61]	[0.28 to 0.47]

Data are presented as "Progression/ Total (Incidence) [95% confidence interval]"

Prediction model C includes IOP, both central ACD and light-room ARA at 750 μm.

PACS= Primary angle closure suspect; PAC= Primary angle closure; IOP=Intraocular pressure; ACD= Anterior chamber depth; ARA= Angle recess area.

eTable 9. Cumulative Incidence Rate and 95% CIs of Progression From PACS to PAC During 14 Years of Follow-Up in Risk Levels Estimated by IOP, Central ACD, Dark-Room TISA at 500 μm, and Prediction Model D

	Risk of progression based on the Prediction model D			
	< 20%	20% to 30%	>30%	Total
Total	26 / 157 (0.17) [0.11 to 0.23]	18 / 102 (0.18) [0.11 to 0.26]	49 / 118 (0.42) [0.33 to 0.51]	93 / 377 (0.25) [0.20 to 0.29]
Risk of progression based on IOP				
< 20% (<13 mmHg)	5 / 56 (0.09) [0.03 to 0.20]	3 / 20 (0.15) [0.03 to 0.38]	2 / 4 (0.50) [0.07 to 0.93]	10 / 80 (0.13) [0.06 to 0.22]
20% to 30% (13 to 17 mmHg)	17 / 89 (0.19) [0.12 to 0.29]	14 / 67 (0.21) [0.12 to 0.33]	28 / 73 (0.38) [0.27 to 0.50]	59 / 229 (0.26) [0.20 to 0.32]
>30% (>17 mmHg)	4 / 12 (0.33) [0.10 to 0.65]	1 / 15 (0.07) [0.01 to 0.32]	19 / 41 (0.46) [0.31 to 0.63]	24 / 68 (0.35) [0.24 to 0.48]
Risk of progression based on central ACD				
< 20% (>2.66 mm)	13 / 95 (0.14) [0.07 to 0.22]	4 / 21 (0.19) [0.05 to 0.42]	0 / 3 (0) [0 to 0.71] [a]	17 / 119 (0.14) [0.09 to 0.22]
20% to 30% (2.43 to 2.66 mm)	11 / 53 (0.21) [0.11 to 0.34]	11 / 54 (0.20) [0.11 to 0.34]	20 / 55 (0.36) [0.24 to 0.50]	42 / 162 (0.26) [0.19 to 0.33]
>30% (<2.43 mm)	2 / 9 (0.22) [0.03 to 0.60]	3 / 27 (0.11) [0.02 to 0.29]	29 / 60 (0.48) [0.35 to 0.62]	34 / 96 (0.35) [0.26 to 0.46]
Risk of progression based on dark-room TISA at 500 μm				
< 20% (>0.06 mm^2)	11 / 78 (0.14) [0.07 to 0.24]	5 / 25 (0.20) [0.07 to 0.41]	2 / 8 (0.25) [0.03 to 0.65]	18 / 111 (0.16) [0.10 to 0.24]
20% to 30% (0.03 to 0.06 mm^2)	12 / 69 (0.17) [0.09 to 0.28]	8 / 48 (0.17) [0.07 to 0.30]	21 / 50 (0.42) [0.28 to 0.57]	41 / 167 (0.25) [0.18 to 0.32]
>30% (<0.03 mm^2)	3 / 10 (0.30) [0.07 to 0.65]	5 / 29 (0.17) [0.06 to 0.36]	26 / 60 (0.43) [0.31 to 0.57]	34 / 99 (0.34) [0.25 to 0.45]

Data are presented as "Progression/ Total (Incidence) [95% confidence interval]"

[a] One-sided, 97.5% confidence interval was provided.

Prediction model D includes IOP, both central ACD and dark-room TISA at 500 μm.

PACS= Primary angle closure suspect; PAC= Primary angle closure; IOP=Intraocular pressure; ACD= Anterior chamber depth; TISA= Trabecular iris space area.

eTable 10. Comparison of Discrimination Abilities Between Baseline Predictors and Prediction Models for the 14-Year Risk of Progression from PACS to PAC

Risk factors and prediction models	AUC (95%CI)	Changes in AUC (95%CI)	
		Compared with IOP	Compared with central ACD
IOP	0.60 (0.53 to 0.66)	-	-0.03 (-0.13 to 0.07)
Central ACD	0.63 (0.56 to 0.70)	0.03 (-0.07 to 0.13)	-
Limbal ACD	0.60 (0.53 to 0.66)	0 (-0.09 to 0.09)	-0.03 (-0.12 to 0.05)
Light-room TISA at 500 μm	0.64 (0.57 to 0.71)	0.05 (-0.05 to 0.14)	0.01 (-0.08 to 0.10)
Light-room ARA at 750 μm	0.63 (0.57 to 0.70)	0.04 (-0.06 to 0.13)	0 (-0.08 to 0.09)
Dark-room TISA at 500 μm	0.62 (0.55 to 0.68)	0.02 (-0.07 to 0.11)	-0.01 (-0.10 to 0.08)
Prediction model A	0.69 (0.63 to 0.75)	0.09 (0.03 to 0.16)	0.06 (0.01 to 0.11)
Prediction model B	0.70 (0.64 to 0.76)	0.11 (0.03 to 0.18)	0.07 (0.02 to 0.13)
Prediction model C	0.70 (0.64 to 0.76)	0.10 (0.03 to 0.18)	0.07 (0.02 to 0.12)
Prediction model D	0.69 (0.62 to 0.75)	0.09 (0.02 to 0.16)	0.06 (0.01 to 0.11)

Risk factors and prediction models	AUC (95%CI)	Changes in AUC (95%CI)	
		Compared with limbal ACD	Compared with light-room TISA at 500 μm
IOP	0.60 (0.53 to 0.66)	0 (-0.09 to 0.09)	-0.05 (-0.14 to 0.05)
Central ACD	0.63 (0.56 to 0.70)	0.03 (-0.05 to 0.12)	-0.01 (-0.10 to 0.08)
Limbal ACD	0.60 (0.53 to 0.66)	-	-0.04 (-0.12 to 0.04)
Light-room TISA at 500 μm	0.64 (0.57 to 0.71)	0.04 (-0.04 to 0.12)	-
Light-room ARA at 750 μm	0.63 (0.57 to 0.70)	0.04 (-0.04 to 0.12)	-0.01 (-0.04 to 0.02)
Dark-room TISA at 500 μm	0.62 (0.55 to 0.68)	0.02 (-0.06 to 0.11)	-0.02 (-0.07 to 0.02)
Prediction model A	0.69 (0.63 to 0.75)	0.09 (0.03 to 0.16)	-
Prediction model B	0.70 (0.64 to 0.76)	-	0.06 (0.01 to 0.11)
Prediction model C	0.70 (0.64 to 0.76)	-	-
Prediction model D	0.69 (0.62 to 0.75)	-	-

Risk factors and prediction models	AUC (95%CI)	Changes in AUC (95%CI)	
		Compared with light-room ARA at 750 μm	Compared with dark-room TISA at 500 μm
IOP	0.60 (0.53 to 0.66)	-0.04 (-0.13 to 0.06)	-0.02 (-0.11 to 0.07)
Central ACD	0.63 (0.56 to 0.70)	0 (-0.09 to 0.08)	0.01 (-0.08 to 0.10)
Limbal ACD	0.60 (0.53 to 0.66)	-0.04 (-0.12 to 0.04)	-0.02 (-0.11 to 0.06)
Light-room TISA at 500 μm	0.64 (0.57 to 0.71)	0.01 (-0.02 to 0.04)	0.02 (- 0.02 to 0.07)
Light-room ARA at 750 μm	0.63 (0.57 to 0.70)	-	0.01 (-0.04 to 0.07)
Dark-room TISA at 500 μm	0.62 (0.55 to 0.68)	-0.01 (-0.07 to 0.04)	-
Prediction model A	0.69 (0.63 to 0.75)	-	-
Prediction model B	0.70 (0.64 to 0.76)	-	-
Prediction model C	0.70 (0.64 to 0.76)	0.07 (0.01 to 0.12)	-
Prediction model D	0.69 (0.62 to 0.75)	-	0.07 (0.01 to 0.12)

Risk factors and prediction models	AUC (95%CI)	Changes in AUC (95%CI)	
		Compared with Prediction model A	Compared with Prediction model B
Prediction model A	0.69 (0.63 to 0.75)	-	-0.01 (- 0.06 to 0.04)
Prediction model B	0.70 (0.64 to 0.76)	0.01 (-0.04 to 0.06)	-
Prediction model C	0.70 (0.64 to 0.76)	0.01 (-0.03 to 0.05)	0 (-0.02 to 0.02)
Prediction model D	0.69 (0.62 to 0.75)	-0.01 (-0.05 to 0.04)	-0.02 (-0.04 to 0.01)

Risk factors and prediction models	AUC (95%CI)	Changes in AUC (95%CI)	
		Compared with Prediction model C	Compared with Prediction model D
Prediction model A	0.69 (0.63 to 0.75)	-0.01 (-0.05 to 0.03)	0.01 (-0.04 to 0.05)
Prediction model B	0.70 (0.64 to 0.76)	0 (-0.02 to 0.02)	0.02 (-0.01 to 0.04)
Prediction model C	0.70 (0.64 to 0.76)	-	0.01 (-0.02 to 0.05)
Prediction model D	0.69 (0.62 to 0.75)	-0.01 (-0.05 to 0.02)	-

Prediction model A includes IOP, central ACD, and limbal ACD; Prediction model B includes IOP, central ACD, and light-room TISA at 500 μm; Prediction model C includes IOP, central ACD, and light-room ARA at 750 μm; Prediction model D includes IOP, central ACD, and dark-room TISA at 500 μm;

PACS= Primary angle closure suspect; PAC= Primary angle closure; AUC= Area under the receiver operating characteristic curve; 95%CI= 95% confidence interval; IOP=Intraocular pressure; ACD= Anterior chamber depth; TISA= Trabecular iris space area; ARA= Angle recess area.

eTable 11. Reclassification for the 14-Year Risk of Progression From PACS to PAC in Prediction Models A, B, C, and D

Prediction model A vs Prediction model B						
Progression risk based on Prediction model A	**Progression risk based on Prediction model B**			**Increased risk**	**Decreased risk**	**Net reclassified**
	<20%	**20% to 30%**	**>30%**			
Eyes with progression from PACS to PAC during the follow-up (N=93)						
<20%	13	7	3			
20% to 30%	5	9	6	16	18	-2
>30%	2	11	37			
Eyes without progression from PACS to PAC during the follow-up (N=284)						
<20%	108	25	2			
20% to 30%	22	41	21	48	47	-1
>30%	4	21	40			
Categorical net reclassification improvement				-0.025 (-0.165 to 0.115)		
Continuous net reclassification improvement				0.159 (-0.074 to 0.393)		
Integrated discrimination improvement				0.015 (-0.007 to 0.037)		

Prediction model A vs Prediction model C						
Progression risk based on Prediction model A	**Progression risk based on Prediction model C**			**Increased risk**	**Decreased risk**	**Net reclassified**
	<20%	**20% to 30%**	**>30%**			
Eyes with progression from PACS to PAC during the follow-up (N=93)						
<20%	15	5	3			
20% to 30%	3	10	7	15	17	-2
>30%	2	12	36			
Eyes without progression from PACS to PAC during the follow-up (N=284)						
<20%	109	25	1			
20% to 30%	25	38	21	47	46	-1
>30%	7	14	44			
Categorical net reclassification improvement				-0.025 (-0.162 to 0.111)		
Continuous net reclassification improvement				0.046 (-0.188 to 0.280)		
Integrated discrimination improvement				0.012 (-0.009 to 0.032)		

Prediction model A vs Prediction model D

Progression risk based on Prediction model A	Progression risk based on Prediction model D			Increased risk	Decreased risk	Net reclassified
	<20%	20% to 30%	>30%			
Eyes with progression from PACS to PAC during the follow-up (N=93)						
<20%	17	5	1			
20% to 30%	7	5	8	14	17	-3
>30%	2	8	40			
Eyes without progression from PACS to PAC during the follow-up (N=284)						
<20%	107	26	2			
20% to 30%	21	40	23	51	42	-9
>30%	3	18	44			
Categorical net reclassification improvement				-0.064 (-0.199 to 0.071)		
Continuous net reclassification improvement				0.031 (-0.203 to 0.265)		
Integrated discrimination improvement				0.009 (-0.011 to 0.029)		

Prediction model B vs Prediction model C

| Progression risk based on Prediction model B	Progression risk based on Prediction model C			Increased risk	Decreased risk	Net reclassified
	<20%	20% to 30%	>30%			
Eyes with progression from PACS to PAC during the follow-up (N=93)						
<20%	16	4	0			
20% to 30%	4	20	3	7	7	0
>30%	0	3	43			
Eyes without progression from PACS to PAC during the follow-up (N=284)						
<20%	126	8	0			
20% to 30%	13	63	11	19	21	2
>30%	2	6	55			
Categorical net reclassification improvement				0.007 (-0.083 to 0.097)		
Continuous net reclassification improvement				-0.073 (-0.306 to 0.160)		
Integrated discrimination improvement				-0.003 (-0.012 to 0.006)		

Prediction model B vs Prediction model D

Progression risk based on Prediction model B	Progression risk based on Prediction model D			Increased risk	Decreased risk	Net reclassified
	<20%	20% to 30%	>30%			
Eyes with progression from PACS to PAC during the follow-up (N=93)						
<20%	20	0	0			
20% to 30%	6	15	6	6	9	-3
>30%	0	3	43			
Eyes without progression from PACS to PAC during the follow-up (N=284)						
<20%	116	18	0			
20% to 30%	15	55	17	35	26	-9
>30%	0	11	52			
Categorical net reclassification improvement				-0.064 (-0.162 to 0.034)		
Continuous net reclassification improvement				-0.067 (-0.301 to 0.167)		
Integrated discrimination improvement				-0.006 (-0.018 to 0.006)		

Prediction model C vs Prediction model D

Progression risk based on Prediction model C	Progression risk based on Prediction model D			Increased risk	Decreased risk	Net reclassified
	<20%	20% to 30%	>30%			
Eyes with progression from PACS to PAC during the follow-up (N=93)						
<20%	17	3	0			
20% to 30%	9	12	6	9	12	-3
>30%	0	3	43			
Eyes without progression from PACS to PAC during the follow-up (N=284)						
<20%	113	23	5			
20% to 30%	18	46	13	41	33	-8
>30%	0	15	51			
Categorical net reclassification improvement				-0.060 (-0.174 to 0.053)		
Continuous net reclassification improvement				-0.098 (-0.330 to 0.135)		
Integrated discrimination improvement				-0.003 (-0.017 to 0.011)		

Prediction model A includes IOP, central ACD, and limbal ACD; Prediction model B includes IOP, central ACD, and light-room TISA at 500 μm; Prediction model C
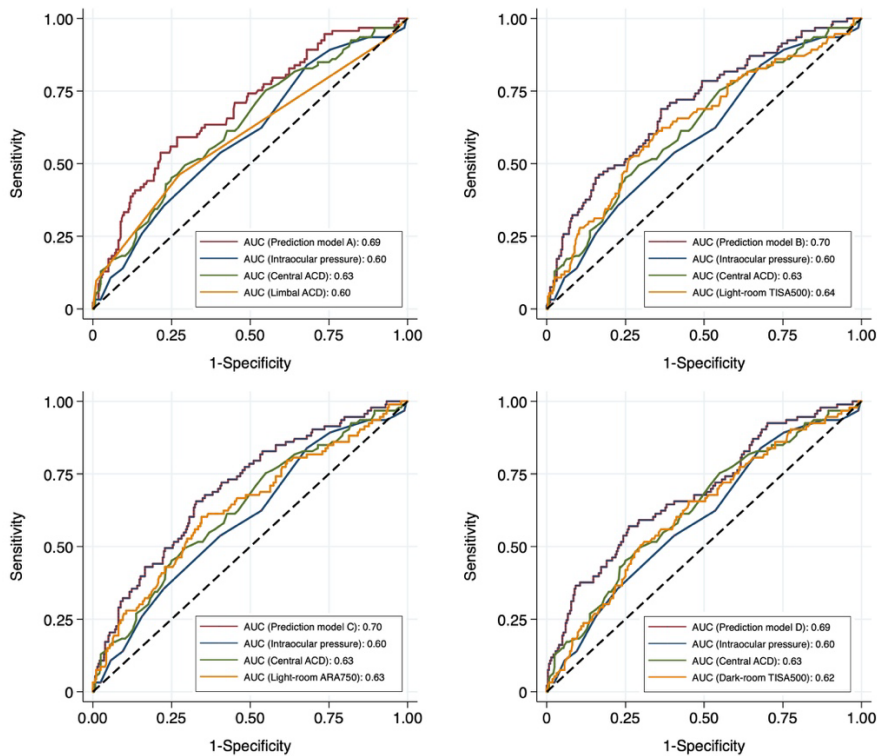
includes IOP, central ACD, and light-room ARA at 750 μm; Prediction model D includes IOP, central ACD, and dark-room TISA at 500 μm;

PACS= Primary angle closure suspect; PAC= Primary angle closure; IOP=Intraocular pressure; ACD= Anterior chamber depth; TISA= Trabecular iris space area; ARA= Angle recess area.

eFigure 1. Anterior Segment Optical Coherence Tomography Metrics Determined by the Zhongshan Angle Assessment Program
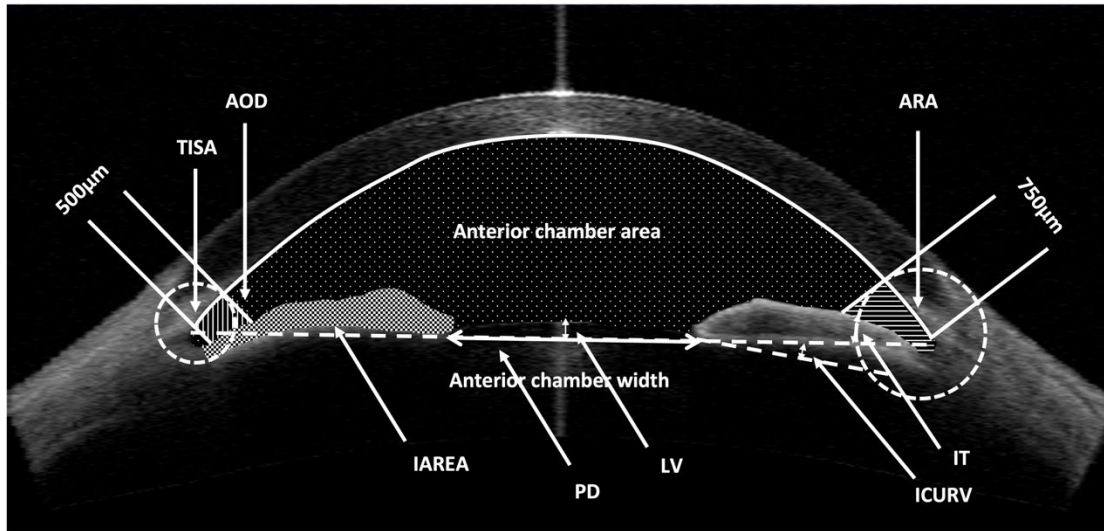

Anterior chamber width: The horizontal distance between two scleral spurs; Lens vault (LV): The perpendicular distance between the anterior surface of lens and the anterior chamber width line; Anterior chamber area: The cross-sectional area bounded by the posterior surface of corneal endothelium, the anterior surface of lens and iris; Pupil diameter (PD): The shortest distance between two pupil edges; Angle open distance at 500μm (AOD): The perpendicular distance between the anterior surface of iris and the trabecular meshwork at 500μm from the scleral spur; Trabecular iris space area at 500μm (TISA): The cross-sectional area bounded by the posterior surface of corneal endothelium, the anterior surface of iris, AOD at 500μm from the scleral spur and the perpendicular distance between the anterior surface of iris and the scleral spur; Angle recess area at 750μm (ARA): The cross-sectional area bounded by the posterior surface of corneal endothelium, the anterior surface of iris and the perpendicular distance between the anterior surface of iris and the trabecular meshwork at 750μm from the scleral spur; Iris thickness at 750μm (IT): The vertical distance from the posterior to the anterior surface of iris at 750μm from the scleral spur; Iris area (IAREA): the total area of iris from the scleral spur to the pupil; Iris curvature (ICURV): the perpendicular distance from iris pigment epithelium at the point of greatest convexity to the line which connects the most central and peripheral points of iris pigment epithelium.

eFigure 2. Receiver Operator Characteristics Curves for the Prediction of Progression from PACS to PAC During 14 Years of Follow-Up

Prediction model A includes IOP, central ACD, and limbal ACD; Prediction model includes IOP, central ACD, and light-room TISA at 500 μm; Prediction model C includes IOP, central ACD, and light-room ARA at 750 μm; Prediction model D includes IOP, central ACD, and dark-room TISA at 500 μm;

PACS=Primary angle closure suspect; PAC=Primary angle closure; AUC= Area under the receiver operating characteristic curve; IOP=Intraocular pressure; ACD=Anterior chamber depth; TISA=Trabecular iris space area; ARA= Angle recess area.

eFigure 3. Calibration Plot Comparing Proportion of Progression From PACS to PAC and 14-Year Risks of Progression Based on Prediction Models A, B, C, and D
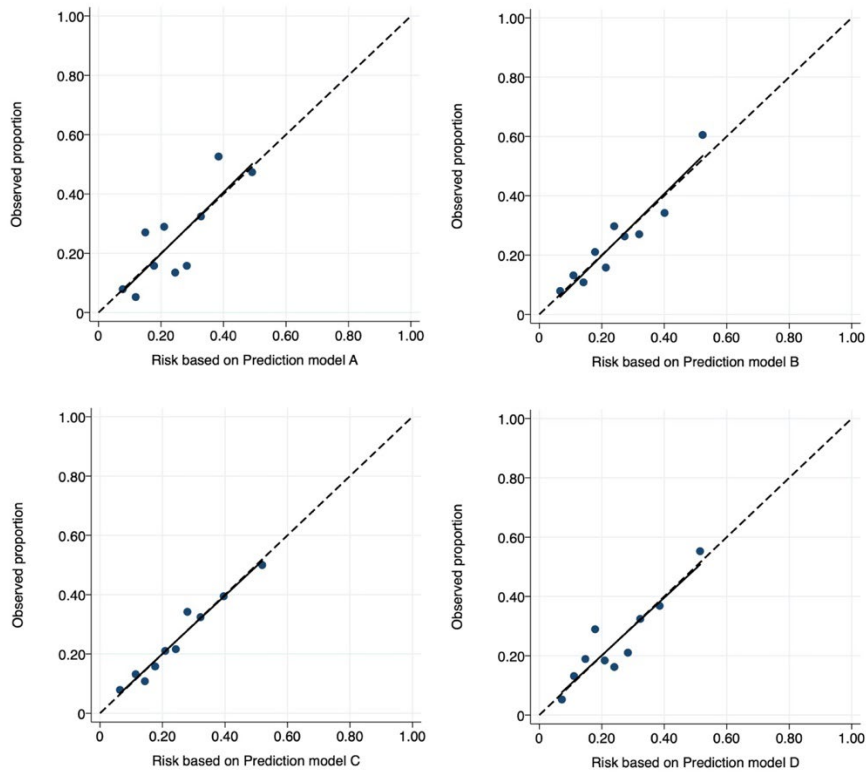
Solid lines represent fitted linear associations between observed proportions and predicted 14-year risks of progression from PACS to PAC.

Prediction model A includes IOP, central ACD, and limbal ACD; Prediction model includes IOP, central ACD, and light-room TISA at 500 μm; Prediction model C includes IOP, central ACD, and light-room ARA at 750 μm; Prediction model D includes IOP, central ACD, and dark-room TISA at 500 μm;

PACS=Primary angle closure suspect; PAC=Primary angle closure; AUC= Area under the receiver operating characteristic curve; IOP=Intraocular pressure; ACD=Anterior chamber depth; TISA=Trabecular iris space area; ARA= Angle recess area.